ChemPubSoc Europe

DOI: 10.1002/cssc.201700576

CHEMSUSCHEM Communications

Renewable Wood Pulp Paper Reactor with Hierarchical Micro/Nanopores for Continuous-Flow Nanocatalysis

Hirotaka Koga,*[a] Naoko Namba,[a] Tsukasa Takahashi,[a] Masaya Nogi,[a] and Yuta Nishina[b]

Continuous-flow nanocatalysis based on metal nanoparticle catalyst-anchored flow reactors has recently provided an excellent platform for effective chemical manufacturing. However, there has been limited progress in porous structure design and recycling systems for metal nanoparticle-anchored flow reactors to create more efficient and sustainable catalytic processes. In this study, traditional paper is used for a highly efficient, recyclable, and even renewable flow reactor by tailoring the ultrastructures of wood pulp. The "paper reactor" offers hierarchically interconnected micro- and nanoscale pores, which can act as convective-flow and rapid-diffusion channels, respectively, for efficient access of reactants to metal nanoparticle catalysts. In continuous-flow, aqueous, room-temperature catalytic reduction of 4-nitrophenol to 4-aminophenol, a gold nanoparticle (AuNP)-anchored paper reactor with hierarchical micro/nanopores provided higher reaction efficiency than state-of-the-art AuNP-anchored flow reactors. Inspired by traditional paper materials, successful recycling and renewal of AuNP-anchored paper reactors were also demonstrated while high reaction efficiency was maintained.

Nanocatalysis, the process of using catalytic metal nanoparticles, has become key technology for effective conversion of a variety of chemicals, because metal nanoparticles can dramatically improve catalytic efficiency through their large surface-area-to-volume ratios and unique electronic properties.[1–3] Recently, nanocatalysis under continuous flow has been recognized as an ideal system for efficient chemical manufacturing.[4–7] Continuous-flow nanocatalysis has clear advantages over conventional batch systems, such as high reaction efficiency, safety, and reproducibility.[8–11] These advantages are consistent with the regulations recently introduced for green sustainable chemistry.[12]

[a] Dr. H. Koga, N. Namba, T. Takahashi, Dr. M. Nogi
The Institute of Scientific and Industrial Research, Osaka University
8-1 Mihogaoka, Ibaraki, Osaka 567-0047 (Japan)
E-mail: hkoga@eco.sanken.osaka-u.ac.jp

[b] Dr. Y. Nishina
Research Core for Interdisciplinary Science, Okayama University
3-1-1 Tsushimanaka, Kita-ku, Okayama 700-8530 (Japan)

Supporting information and the ORCID identification number(s) for the author(s) of this article can be found under https://doi.org/10.1002/cssc.201700576.

Metal nanoparticle catalysts anchored within flow reactors can serve as an excellent platform for continuous-flow nanocatalysis, because there is no contamination by catalysts in the products.[5,6,13,14] One of the current challenges in creating more efficient chemical manufacturing processes is in designing the porous structure of flow reactors. Porous structures inside flow reactors can act as flow channels and control the access of reactants to catalysts anchored within the reactors, determining reaction efficiency in practice. In this regard, the development of flow reactors with tailored porous channels has become a major center of attraction and a variety of flow reactors with microscale or nanoscale pores, based on anodic alumina membranes,[4] ceramic membranes,[15] silica nanosprings,[16] silica monoliths,[17] glass fibers,[18] and synthetic polymers,[19] have been investigated. However, the design of nanoscale and microscale porous structures inside flow reactors remains challenging for optimizing access of reactants to catalysts for further improvement of reaction efficiency. From the viewpoints of eco-friendliness and sustainability, a system for effective recycling of metal nanoparticle catalyst-anchored flow reactors is also essential, particularly because metal nanoparticle catalysts are expensive and a limited resource.[20,21]

As mentioned above, there is a growing need for highly efficient continuous-flow nanocatalysis with an excellent recycling system for truly green sustainable chemistry. To achieve this challenge, paper, which has been used traditionally on a daily basis, is expected to offer great potential for use as an efficient and recyclable flow reactor, because it has highly porous structures, a high absorption capacity for liquids, high stability in most solvents, is both hydrophilic and lipophilic nature, and is recyclable.[22–36] Paper is composed of wood pulp fibers several tens of μm in width, which are derived from wood cells. Wood pulp has hierarchical micro/nanostructures (see the Supporting information, Figure S1 a); it is a hollow fiber with a microscale inner pore (lumen), and its wall consists of bundles of cellulose nanofibrils (nanocellulose) with widths from 3 to several tens of nm.[37,38] Although traditional paper contains microscale pores derived from both the hollow and network structures of wood pulp, denoted pulp networks, further tailoring of the nanostructures derived from the nanocellulose networks in the wall of wood pulp can provide opportunities to broaden the potential of paper as a new class of flow reactors with recyclability.

Herein, we report a highly efficient, recyclable, and even renewable paper reactor for continuous-flow nanocatalysis. The paper reactor was constructed by assembly of wood pulp with tailored nanoscale pores in its walls. Then, hierarchically interconnected micro- and nanoscale pores were derived from the pulp and nanocellulose networks, respectively (Figure S1 b).

The wood-derived and well-designed porous structures inside the paper reactor can provide effective access of reactants to embedded metal nanoparticle catalysts. As a proof-of-concept demonstration, a gold nanoparticle (AuNP)-anchored paper reactor achieved efficient continuous-flow nanocatalysis for the aqueous-phase, room-temperature reduction of 4-nitrophenol to 4-aminophenol. The turnover frequency (TOF) was up to 440 h^{-1}, which is higher than values obtained in state-of-the-art AuNP-anchored flow reactors. Excellent recyclability and renewability for AuNP-anchored paper reactors were also demonstrated, opening new doors for the development of highly efficient, green, and sustainable chemistry.

Prior to fabrication of the paper reactor, anchoring of AuNP catalysts in wood pulp was conducted, followed by tailoring of nanoscale pores in the walls of the wood pulp. First, AuNPs were synthesized in situ within wood pulp by using polyethylenimine (PEI) as both an adsorbent and reductant for Au precursor ions ($[AuCl_4]^-$), as follows. An aqueous suspension of never-dried wood pulp, with weakly negative charge,[39] was mixed with an aqueous solution of PEI containing a high density of positive charge to afford positively charged pulp. Subsequently, negatively charged Au precursor ions were attached to the positively charged pulp through electrostatic interaction, followed by dewatering and thermal treatment at 110 °C for 30 min. The as-prepared pulp had a hollow structure with microscale inner pores (Figure 1 a,b). The formation of crystalline AuNPs with a crystallite size of 2.4 nm on the surface of the pulp wall was then confirmed (Figure 1 c,g; see also Figure S2). AuNPs were successfully formed through PEI-mediated reduction of the Au precursor ions.[40] In this case, however, dense nanostructures derived from nanocellulose fibers were observed on the wall surfaces of the pulp (Figure 1 c), suggesting that the nanocellulose fibers became unavoidably agglomerated during the drying process in the presence of water, because of the high surface tension of water (72.14 $mN\,m^{-1}$ at 25 °C),[41] as in the Campbell effect.[42] In this study, therefore, solvent exchange from water to *tert*-butyl alcohol (*t*BuOH), which has a low surface tension (19.96 $mN\,m^{-1}$ at 25 °C),[41] was conducted before the drying process to suppress the nanocellulose packing. The resulting pulp formed nanoscale pores derived from the nanocellulose networks in its wall (Figure 1 d–f), within which AuNPs were dispersed and anchored. The specific surface area of the AuNPs-anchored pulp was thereby increased from about 0.5 to 20 $m^2\,g^{-1}$ by solvent exchange with *t*BuOH, also indicating the formation of nanoscale pores (Figure 1 h). Thus, AuNP-anchored pulp, incorporating both microscale inner pores and nanoscale pores tailored in its wall, was successfully prepared by a simple *t*BuOH treatment.

Subsequently, the AuNP-anchored pulp with nanoscale pores was fabricated into a paper material, i.e., a paper reactor, using a facile papermaking process. Although traditional pulp paper is white, the as-prepared paper reactor was uniformly pink because of the surface plasmon resonance of AuNPs (Figure 2 a),[43] indicating that AuNP catalysts were well dispersed in the paper reactor. The AuNP-anchored paper reactor had microscale pores with sizes of 0.1–100 μm, derived from both

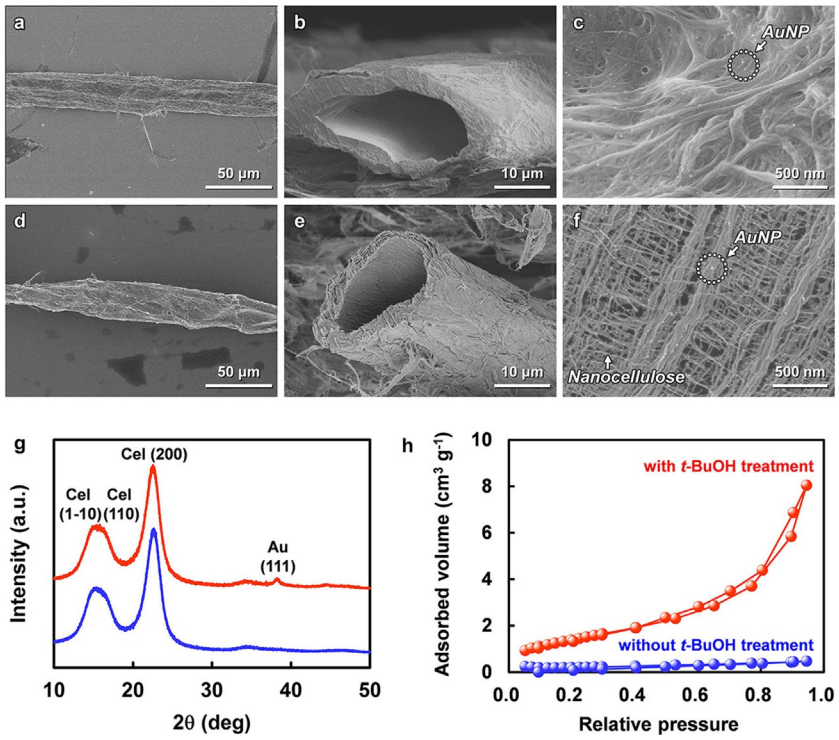

Figure 1. AuNP-anchored wood pulp with tailored nanostructures. a–f) Field-emission scanning electron microscope (FE-SEM) images of the AuNP-anchored pulp prepared without (a–c) and with (d–f) solvent exchange treatment using *t*BuOH. a, d) Top-view, b, e) cross-section, and c, f) wall surface of the AuNP-anchored pulp. g) X-ray diffraction (XRD) patterns of the pulp (blue) and the AuNP-anchored pulp (red). h) Nitrogen adsorption-desorption isotherms of the AuNP-anchored pulp prepared without (blue) and with (red) *t*BuOH treatment.

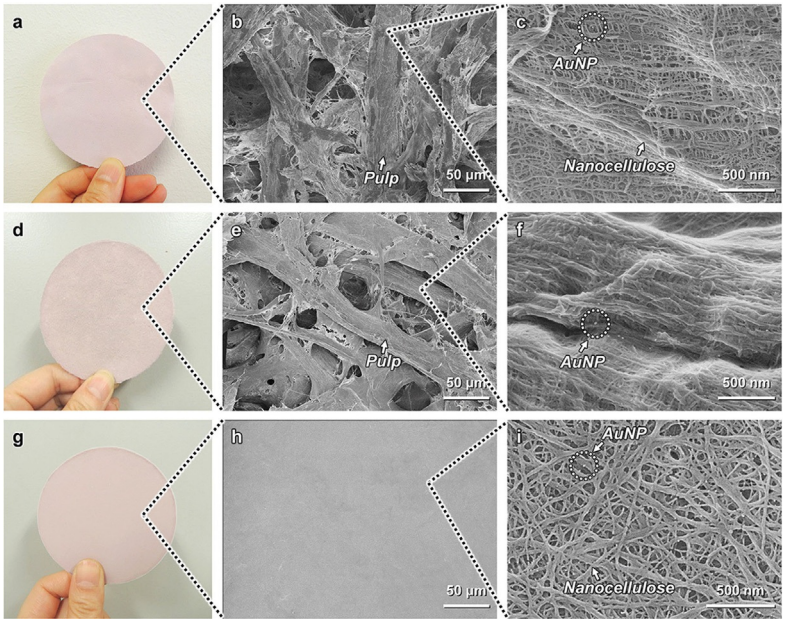

Figure 2. AuNP-anchored paper reactors with tailored porous structures. Optical (a, d, g) and FE-SEM (b, c, e, f, h, i) images of AuNP-anchored paper reactors with different pore structures. a–c) AuNP-anchored paper reactor with micro/nanoscale pores fabricated from the AuNP-anchored pulp with nanoscale pores (with *t*BuOH treatment). d–f) AuNP-anchored paper reactor containing only microscale pores fabricated from the AuNP-anchored pulp without nanoscale pores (without *t*BuOH treatment). g–i) AuNP-anchored paper reactor containing only nanoscale pores fabricated from the AuNP-anchored nanocellulose with *t*BuOH treatment, instead of AuNP-anchored pulp.

the hollow (Figure 1e) and network structures of the pulp (Figure 2b), i.e., pulp networks, in addition to nanoscale pores with sizes of 4–100 nm, derived from the nanocellulose networks in the wall of the pulp (Figure 2c; see also Figure S3). Thus, an AuNP-anchored paper reactor with hierarchically interconnected micro/nanoscale pores was successfully fabricated. The grammage of the AuNP-anchored paper reactor with micro/nanoscale pores was about 69 g m^{-2} and the contents of pulp, PEI, and AuNP were 98.5 wt%, 1.3 wt%, and 0.2 wt%, respectively. As a control sample, an AuNP-anchored paper reactor containing only microscale pores was fabricated from AuNP-anchored pulp without nanoscale pores (Figure 2d–f; see also Figure S3), through preparation without *t*BuOH treatment. An AuNP-anchored paper reactor containing only nanoscale pores was also fabricated using AuNP-anchored nanocellulose treated with *t*BuOH, instead of the AuNP-anchored pulp (Figure 2g–i; see also Figure S3).

The as-prepared AuNP-anchored paper reactors were subjected to continuous-flow nanocatalysis for aqueous room-temperature reduction of 4-nitrophenol, which is a common environmental pollutant, with sodium borohydride ($NaBH_4$) to 4-aminophenol, which is an important intermediate for the manufacture of pharmaceuticals. For continuous-flow nanocatalysis, the AuNP-anchored paper reactor was cut into circular discs with a diameter of about 9.0 mm, then vertically stacked and tightly packed into a syringe equipped with a silicon tube. In all cases, the length and volume of the paper layer were set at about 1.75 mm and 110 mm^3, respectively. The reaction solution was then fed into the syringe (Figure 3a, b). Figure 3c shows the UV/Vis spectra of a 50 μM 4-nitrophenol solution with 50 mM $NaBH_4$ before and after feeding into the AuNP anchored paper reactor containing micro/nanoscale pores at 0.05 mL min^{-1}. After feeding, the characteristic peak for 4-nitrophenol at 400 nm, assigned to the 4-nitrophenolate ion,[44] disappeared, while a new peak at 300 nm, ascribed to 4-aminophenol,[44] appeared. The absorbance at 300 nm was then approximately equal to that of 50 μM 4-aminophenol solution, suggesting that the AuNP-anchored paper reactor with micro/nanoscale pores achieved almost 100% conversion of 4-nitrophenol to 4-aminophenol.

When the AuNP-free paper reactor was used with $NaBH_4$ and when the AuNP-anchored paper reactor was used without $NaBH_4$, the reaction did not proceed at all, indicating that AuNPs and $NaBH_4$ played an essential role as a catalyst and a reducing agent, respectively, and that PEI and wood pulp paper had no catalytic activity during 4-nitrophenol reduction (Figure S4). In addition, there was almost no adsorption of either 4-nitrophenol or 4-aminophenol on the paper reactor, indicating that wood pulp paper did not inhibit the 4-nitrophenol reduction reaction in an aqueous system (Figure S4). However, the actual reaction efficiencies clearly depended on the porous structures within the paper (Figure 3d). It should be noted that the AuNP-anchored paper reactor with micro/nanoscale pores (Figure 2a–c) demonstrated much higher reaction efficiency at all feed rates than those containing only microscale (Figure 2d–f) or nanoscale pores (Figure 2g–i), while reducing the AuNP catalyst usage to two thirds. The TOF value (the amount of product obtained per unit time per unit amount of catalyst) of the AuNPs-anchored paper reactor with micro/nanoscale pores reached 440 h^{-1} (Figure S5), which is superior to the TOF values of state-of-the-art flow reactors that are based on inorganic and organic materials (Figure 3e; see

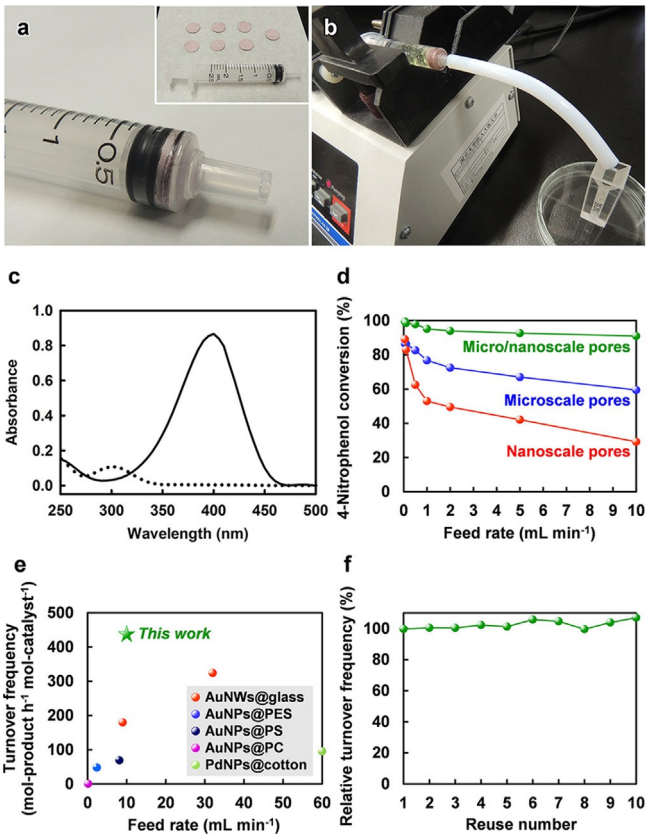

Figure 3. Continuous-flow nanocatalysis by the AuNP-anchored paper reactors. Typical reactor setup using a packed syringe containing the AuNP-anchored paper reactor (a) and a syringe pump (b) for aqueous room-temperature reduction of 4-nitrophenol to 4-aminophenol. c) UV/Vis absorption spectra of a 50 μM 4-nitrophenol solution with 50 mM $NaBH_4$ before (solid line) and after (dotted line) feeding into the AuNP-anchored paper reactor with micro/nanoscale pores at 0.05 mL min^{-1}. d) 4-Nitrophenol conversion versus feed rate for AuNP-anchored paper reactors containing different porous structures. e) TOF value versus feed rate for state-of-the-art flow reactors in the 4-nitrophenol reduction. f) Relative TOF versus reuse number for the AuNP-anchored paper reactor with micro/nanoscale pores. Au catalyst content in the paper reactor: 0.45 μmol per 110 mm^3 (microscale pores, nanoscale pores) and 0.30 μmol per 110 mm^3 (micro/nanoscale pores).

also Table S1). In other words, the catalytic performance of the AuNP-anchored paper reactor with micro/nanoscale pores was higher than those of various flow reactors based on Au nanowire-anchored glass fibers (AuNWs@glass),[18] AuNP-anchored polyethersulfone hollow fiber membranes (AuNPs@PES),[19] AuNP-anchored polysulfone hollow fiber membranes (AuNPs@PS),[19] AuNP-anchored polycarbonate membranes (AuNPs@PC),[45] and palladium nanoparticle-anchored cotton fibers (PdNPs@cotton).[46] Paper is easy to handle and can be reused after the catalytic reaction; Zheng et al. recently reported good reusability of the Pd-loaded cellulose filter paper for cross-coupling reactions in batch system.[47] In this study, Au leaching from the AuNP-anchored paper reactor after the flow reaction was not detected by atomic absorption analysis, and the AuNP-anchored paper reactor with micro/nanoscale pores could be reused for at least ten successive runs without a loss in catalytic efficiency (Figure 3 f). These results suggest that the wood pulp paper reactor with tailored flow-through pores (Figure S1 b) is a promising candidate for the continuous production of useful chemicals through the use of highly efficient flow nanocatalysis.

To explain the mechanism behind the high reaction efficiency of the AuNP-anchored paper reactor with micro/nanoscale pores, the respective roles of microscale and nanoscale pores as flow channels are discussed below. Nanoscale pores can act as fast-diffusion channels for rapid access of reactants to catalysts, because the typical diffusion time scale τ in nanoscale pores is considered to be 10^6 times smaller than that in microscale pores ($\tau = l^2 2D^{-1}$, where l is the diffusion length and D is the diffusion coefficient).[17] In practice, nanoscale pores were more efficient than microscale pores at feed rates below 0.05 mL min^{-1} (Figure 3 d). However, nanoscale pores showed a drastic decrease in reaction efficiency with increasing feed rate, resulting in lower efficiencies than microscale pores at higher feed rates (Figure 3 d). To elucidate this phenomenon, we investigated the effect of porous structures within the paper reactor on flow uniformity of the reactants at a feed rate of 0.05 or 10 mL min^{-1} (Figure S6). At each feed rate, there was no difference in the residence time of reactants in the paper layer among the paper reactors, regardless of their porous structures, indicating good permeability. However, the flow uniformity in the paper reactors varied with their porous structures; whereas small nanoscale pores caused non-uniform flow distribution in the paper reactor, possibly due to local flow (i.e., channeling phenomenon), relatively large microscale pores allowed uniform flow distribution (Figure S6 d). From these results, it was speculated that nanoscale pores allow fast diffusion of reactants but cause inefficient access of reactants to the AuNP catalyst owing to non-uniform flow distribution, resulting in relatively low reaction efficiency, especially at high feed rates. Meanwhile, micro/nanoscale pores would offer both uniform flow and fast diffusion of reactants. Thus, it was suggested that the tailored micro/nanoscale pores can provide both effective convective-flow channels and fast-diffusion channels for efficient access of reactants to the AuNP catalyst, leading to an enhanced reaction efficiency.

Although continuous-flow nanocatalysis may be an ideal system for effective chemical manufacturing, recycling and renewal of the conventional metal nanoparticle catalyst-anchored flow reactors remain a challenge for realizing green sustainable chemistry. The AuNP-anchored paper reactor had enough mechanical stability to be recovered after use in continuous-flow nanocatalysis at a feed rate of 10 mL min^{-1}, and was also able to overcome this challenge by taking advantage of paper-specific recyclability. The AuNP-anchored paper reactor with micro/nanoscale pores was renewable beyond the point of mere recyclability (Figure 4 a). First, the AuNPs-anchored paper reactor was thoroughly washed with distilled water after use in continuous-flow nanocatalysis and then immersed in aqua regia at room temperature for several seconds to elute Au ions from the paper reactor. The resulting paper was thoroughly washed with distilled water and then sonicated to prepare an aqueous suspension of the recycled pulp. The solution of the eluted Au ions was then neutralized by using an aqueous solution of sodium hydroxide. Thus, the AuNP-anchored

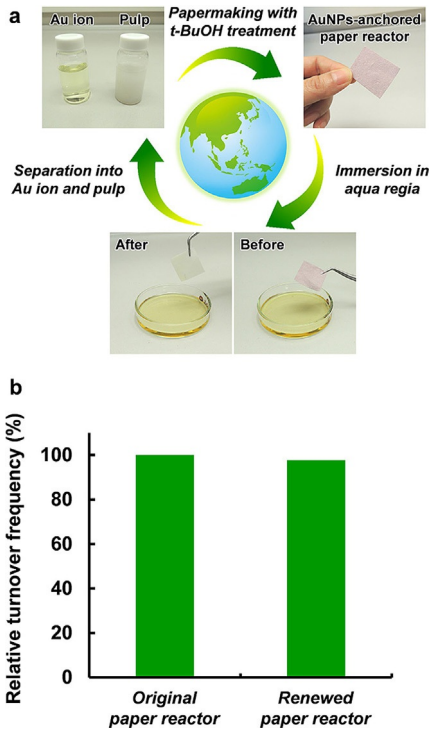

Figure 4. Recyclability and renewability of the AuNP-anchored paper reactor: a) Schematic of a typical recycling and renewing system for the AuNP-anchored paper reactor with micro/nanoscale pores. b) Reaction efficiency of the renewed AuNP-anchored paper reactor with micro/nanoscale pores at a feed rate of 10 mL min^{-1}.

paper reactor was separated into the recycled Au ions and pulp. Finally, the recycled Au ions and pulp were fabricated into the AuNP-anchored paper reactor using the papermaking process with *t*BuOH treatment. The renewed AuNP-anchored paper reactor maintained its specific micro/nanoscale pores, the crystalline structure of native cellulose (Figure S7), and high reaction efficiency (Figure 4b), indicating the feasibility of truly sustainable continuous-flow nanocatalysis.

To demonstrate the broad application of our paper reactor, we investigated the anchoring of other metal NPs for fine chemical production. Pd is one of the most popular catalysts to produce useful chemicals, such as pharmaceuticals, agrochemicals, and cosmetics, through cross-coupling reactions. A PdNP-anchored paper reactor with micro/nanoscale pores was prepared by using a similar process to that for the AuNP-anchored reactor (Figure S8) and used for cross-coupling reaction of aryl iodide with alkyllithium reagent (Scheme 1); it achieved almost 100% conversion of 4-iodotoluene at room temperature and with a feed rate of 0.2 mL min^{-1}. Although a similar type of reaction in batch system using a Pd^0 complex with

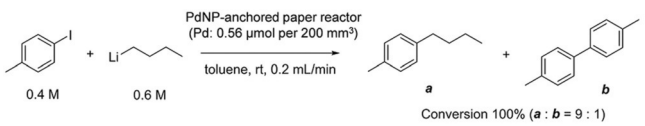

Scheme 1. Cross-coupling of 4-iodotoluene and *n*BuLi.

phosphine ligand was recently reported,[48] the PdNP-anchored paper reactor is expected to enable a continuous-flow and heterogeneous analogue of such a cross-coupling reaction without any phosphine ligand.

In summary, we demonstrated highly efficient continuous-flow nanocatalysis with an excellent recycling system, based on an AuNP-anchored paper reactor. The paper reactor contained hierarchical micro/nanoscale flow-through pores tailored from wood pulp, boosting reaction efficiency while reducing the use of AuNPs. Furthermore, successful reuse, recycling, and renewing of the AuNP-anchored paper reactor were demonstrated. Thus, the AuNPs-anchored paper reactor provides good opportunities to support green processing by reducing catalyst wastage, reuse, recycling, and renewing, while also achieving effective production of useful chemicals. The paper reactor can be prepared from ubiquitous and abundant wood resources through large-area mass production such as the well-established papermaking process. This novel strategy can be extended to various other metal nanoparticle catalysts and corresponding chemical reactions, and enables facile, highly efficient, and truly sustainable chemical manufacturing using paper.

Acknowledgements

Never-dried softwood pulp was kindly provided by Nippon Paper Industries Co., Ltd., Japan. The authors wish to thank Dr. Shuren Cong for his assistance in XPS analyses. H.K. was partially supported by Grants-in-Aid for Scientific Research (Grant No. 26660144 and 15H05627) from the Japan Society for the Promotion of Science and by the Cooperative Research Program "CORE Lab" of Network Joint Research Center for Materials and Devices: Dynamic Alliance for Open Innovation Bridging Human, Environment and Materials.

Conflict of interest

The authors declare no conflict of interest.

Keywords: continuous flow · gold · heterogeneous catalysis · microreactors · paper

[1] M. Haruta, *Nature* **2005**, *437*, 1098 – 1099.
[2] J. M. Campelo, D. Luna, R. Luque, J. M. Marinas, A. A. Romero, *ChemSusChem* **2009**, *2*, 18 – 45.
[3] *Nanocatalysis: Synthesis and Applications* (Eds.: V. Polshettiwar, T. Asefa), Wiley, Hoboken, NJ, **2013**.
[4] D. M. Dotzauer, J. Dai, L. Sun, M. L. Bruening, *Nano Lett.* **2006**, *6*, 2268 – 2272.
[5] R. Ricciardi, J. Huskens, W. Verboom, *ChemSusChem* **2015**, *8*, 2586 – 2605.
[6] T. Tsubogo, H. Oyamada, S. Kobayashi, *Nature* **2015**, *520*, 329 – 332.
[7] R. Porta, M. Benaglia, A. Puglisi, *Org. Process Res. Dev.* **2016**, *20*, 2 – 25.
[8] C. Wiles, P. Watts, *Green Chem.* **2012**, *14*, 38 – 54.
[9] S. V. Ley, I. R. Baxendale, *Nat. Rev. Drug Discovery* **2002**, *1*, 573 – 586.
[10] K. Geyer, J. D. C. Codée, P. H. Seeberger, *Chem. Eur. J.* **2006**, *12*, 8434 – 8442.
[11] R. L. Hartman, J. P. McMullen, K. F. Jensen, *Angew. Chem. Int. Ed.* **2011**, *50*, 7502 – 7519; *Angew. Chem.* **2011**, *123*, 7642 – 7661.

[12] P. T. Anastas, J. C. Warner, *Green Chemistry: Theory and Practice*, Oxford University Press, Oxford, **1998**.
[13] C. V. Navin, K. S. Krishna, C. S. Theegala, C. S. S. R. Kumar, *Nanotechnol. Rev.* **2013**, *3*, 39 – 63.
[14] E. Shahbazali, V. Hessel, T. Noël, Q. Wang, *Nanotechnol. Rev.* **2013**, *3*, 65 – 86.
[15] N. Wehbe, N. Guilhaume, K. Fiaty, S. Miachon, J.-A. Dalmon, *Catal. Today* **2010**, *156*, 208 – 215.
[16] K. F. Schilke, K. L. Wilson, T. Cantrell, G. Corti, D. N. McIlroy, C. Kelly, *Biotechnol. Prog.* **2010**, *26*, 1597 – 1605.
[17] A. E. Kadib, R. Chimenton, A. Sachse, F. Fajula, A, Galarneau, B. Coq, *Angew. Chem. Int. Ed.* **2009**, *48*, 4969 – 4972; *Angew. Chem.* **2009**, *121*, 5069 – 5072.
[18] J. He, W. Ji, L. Yao, Y. Wang, B. Khezri, R. D. Webster, H. Chen, *Adv. Mater.* **2014**, *26*, 4151 – 4155.
[19] L. Ouyang, D. M. Dotzauer, S. R. Hogg, J. Macanás, J.-F. Lahitte, M. L. Bruening, *Catal. Today* **2010**, *156*, 100 – 106.
[20] C. Pavia, E. Ballerini, L. A. Bivona, F. Giacalone, C. Aprile, L. Vaccaro, M. Gruttadauria, *Adv. Synth. Catal.* **2013**, *355*, 2007 – 2018.
[21] C. Petrucci, G. Strappaveccia, F. Giacalone, M. Gruttadauria, F. Pizzo, L. Vaccaro, *ACS Sustainable Chem. Eng.* **2014**, *2*, 2813 – 2819.
[22] V. Leung, A.-A. M. Shehata, C. D. M. Filipe, R. Pelton, *Colloids Surf. A* **2010**, *364*, 16 – 18.
[23] S. Jahanshahi-Anbuhi, P. Chavan, C. Sicard, V. Leung, S. M. Z. Hossain, R. Pelton, J. D. Brennan, C. D. M. Filipe, *Lab Chip* **2012**, *12*, 5079 – 5085.
[24] J. Wang, D. Bowie, X. Zhang, C. Filipe, R. Pelton, J. D. Brennan, *Chem. Mater.* **2014**, *26*, 1941 – 1947.
[25] X. Li, D. R. Ballerini, W. Shen, *Biomicrofluidics* **2012**, *6*, 011301.
[26] D. R. Ballerini, X. Li, W. Shen, *Microfluid. Nanofluid.* **2012**, *13*, 769 – 787.
[27] A. Böhm, M. Gattermayer, C. Trieb, S. Schabel, D. Fiedler, F. Miletzky, M. Biesalski, *Cellulose* **2013**, *20*, 467 – 483.
[28] A. Böhm, F. Carstens, C. Trieb, S. Schabel, M. Biesalski, *Microfluid. Nanofluid.* **2014**, *16*, 789 – 799.
[29] S. Bump, A. Böhm, L. Babel, S. Wendenburg, F. Carstens, S. Schabel, M. Biesalski, T. Meckel, *Cellulose* **2015**, *22*, 73 – 88.
[30] E. Fu, P. Kauffman, B. Lutz, P. Yager, *Sens. Actuators B* **2010**, *149*, 325 – 328.
[31] E. Fu, B. Lutz, P. Kauffman, P. Yager, *Lab Chip* **2010**, *10*, 918 – 920.
[32] E. Fu, T. Liang, J. Houghtaling, S. Ramachandran, S. A. Ramsey, B. Lutz, P. Yager, *Anal. Chem.* **2011**, *83*, 7941 – 7946.
[33] H. Koga, T. Kitaoka, A. Isogai, *J. Mater. Chem.* **2011**, *21*, 9356 – 9361.
[34] H. Koga, T. Kitaoka, A. Isogai, *J. Mater. Chem.* **2012**, *22*, 11591 – 11597.
[35] H. Koga, T. Kitaoka, A. Isogai, *Molecules* **2015**, *20*, 1495 – 1508.
[36] M. O. Rahman, A. Hussain, H. Basri, *Int. J. Environ. Sci. Technol.* **2014**, *11*, 551 – 564.
[37] J. Fahlén, Ph.D. Thesis, KTH Royal Institute of Technology, Stockholm, Sweden **2005**.
[38] G. Chinga-Carrasco, *Nanoscale Res. Lett.* **2011**, *6*, 417 – 423.
[39] H. Koga, H. Tonomura, M. Nogi, K. Suganuma, Y. Nishina, *Green Chem.* **2016**, *18*, 1117 – 1124.
[40] T. Zhang, W. Wang, D. Zhang, X. Zhang, Y. Ma, Y. Zhou, L. Qi, *Adv. Funct. Mater.* **2010**, *20*, 1152 – 1160.
[41] J. J. Jasper, *J. Phys. Chem. Ref. Data* **1972**, *1*, 841 – 1009.
[42] W. B. Campbell, *Tappi J.* **1959**, *42*, 999 – 1001.
[43] S. K. Ghosh, T. Pal, *Chem. Rev.* **2007**, *107*, 4797 – 4862.
[44] K. Kuroda, T. Ishida, M. Haruta, *J. Mol. Catal. A* **2009**, *298*, 7 – 11.
[45] A. S. Peinetti, L. P. M. De Leo, G. A. González, F. Battaglini, *J. Colloid Interface Sci.* **2012**, *386*, 44 – 50.
[46] J. Xi, J. Xiao, F. Xiao, Y. Jin, Y. Dong, F. Jing, S. Wang, *Sci. Rep.* **2016**, *6*, 21904.
[47] G. Zheng, K. Kaefer, S. Mourdikoudis, L. Polavarapu, B. Vaz, S. E. Cartmell, A. Bouleghlimat, N. J. Buurma, L. Yate, Á. R. de Lera, L. M. Liz-Marzán, I. Pastoriza-Santos, J. Pérez-Juste, *J. Phys. Chem. Lett.* **2015**, *6*, 230 – 238.
[48] M. Giannerini, M. Fañanás-Mastral, B. L. Feringa, *Nat. Chem.* **2013**, *5*, 667 – 672.

Manuscript received: April 6, 2017
Accepted manuscript online: October 4, 2017
Version of record online: May 4, 2017

